frontiers | Frontiers in Chemistry

ORIGINAL RESEARCH
published: 16 June 2022
doi: 10.3389/fchem.2022.868794

Electrospun Ta-MOF/PEBA Nanohybrids and Their CH_4 Adsorption Application

Saade Abdalkareem Jasim[1], *Jihad M. Hadi*[2], *Abduladheem Turki Jalil*[3], *Maria Jade Catalan Opulencia*[4], *Ali Thaeer Hammid*[5], *Mohadeseh Tohidimoghadam*[6]* and *Mohammadreza Moghaddam-manesh*[7]

[1]Medical Laboratory Techniques Department, Al-Maarif University College, Ramadi, Iraq, [2]Department of Medical Laboratory of Science, College of Health Sciences, University of Human Development, Kurdistan Regional Government, Slemani, Iraq, [3]Medical Laboratories Techniques Department, Al-Mustaqbal University College, Hilla, Iraq, [4]College of Business Administration, Ajman University, Ajman, United Arab Emirates, [5]Computer Engineering Techniques Department, Faculty of Information Technology, Imam Ja'afar Al-Sadiq University, Baghdad, Iraq, [6]Pasteur Hospital, Bam University of Medical Science, Bam, Iran, [7]Petrochemistry and Polymer Research Group, Chemistry and Petrochemistry Research Center, Standard Research Institute, Karaj, Iran

OPEN ACCESS

Edited by:
Manoj B. Gawande, Palacky University Olomouc, Czechia

Reviewed by:
Deng-Guang Yu, University of Shanghai for Science and Technology, China
Izabela S.Pieta, Institute of Physical Chemistry (PAN), Poland

***Correspondence:**
Mohadeseh Tohidimoghadam mohadesehtohidimoghadam@gmail.com

Specialty section:
This article was submitted to Green and Sustainable Chemistry, a section of the journal Frontiers in Chemistry

Received: *04 February 2022*
Accepted: *09 May 2022*
Published: *16 June 2022*

Citation:
Jasim SA, Hadi JM, Jalil AT, Catalan Opulencia MJ, Hammid AT, Tohidimoghadam M and Moghaddam-manesh M (2022) Electrospun Ta-MOF/PEBA Nanohybrids and Their CH_4 Adsorption Application. Front. Chem. 10:868794. doi: 10.3389/fchem.2022.868794

For the first time, biocompatible and biodegradable Ta-metal organic framework (MOF)/polyether block amide (PEBA) fibrous polymeric nanostructures were synthesized by ultrasonic and electrospinning routes in this study. The XRD peaks of products were wider, which is due to the significant effect of the ultrasonic and electrospinning methods on the final product. The adsorption/desorption behavior of the nanostructures is similar to that of the third type of isotherm series, which showed mesoporous behavior for the products. The sample has uniform morphology without any evidence of agglomeration. Since the adsorption and trapping of gaseous pollutants are very important, the application of the final Ta-MOF/PEBA fibrous polymeric nanostructures was investigated for CH_4 adsorption. In order to achieve the optimal conditions of experiments and also systematic studies of the parameters, fractional factorial design was used. The results showed that by selecting temperature 40°C, time duration 35 min, and pressure 3 bar, the CH_4 gas adsorption rate was near 4 mmol/g. Ultrasonic and electrospinning routes as well as immobilization of Ta-MOF in the PEBA fibrous network affect the performance of the final products for CH_4 gas adsorption.

Keywords: Ta-MOF/PEBA, ultrasonic-assisted electrospinning, CH_4 adsorption, fibrous polymer, air pollution

1 INTRODUCTION

In recent years, due to the expansion of industries, gaseous pollutants have increased significantly (Zheng et al., 2018). The effects of these pollutants have become so severe that reducing them has attracted the attention of communities and organizations (Afroz et al., 2003). One of the gas pollutants that has adverse effects on the environment, plants, and animals is CH_4 (Van Amstel, 2012). Due to its harmful momentary effects, trapping CH_4 using a desirable device is very important and critical (Murseli et al., 2019).

In the last few years, different nanostructures such as active carbon and zeolite have been studied in the field of CH_4 gas adsorption due to their desirable potential properties (Rios et al., 2013; Mofarahi and Gholipour, 2014). Recently, metal organic frameworks (MOFs) have been

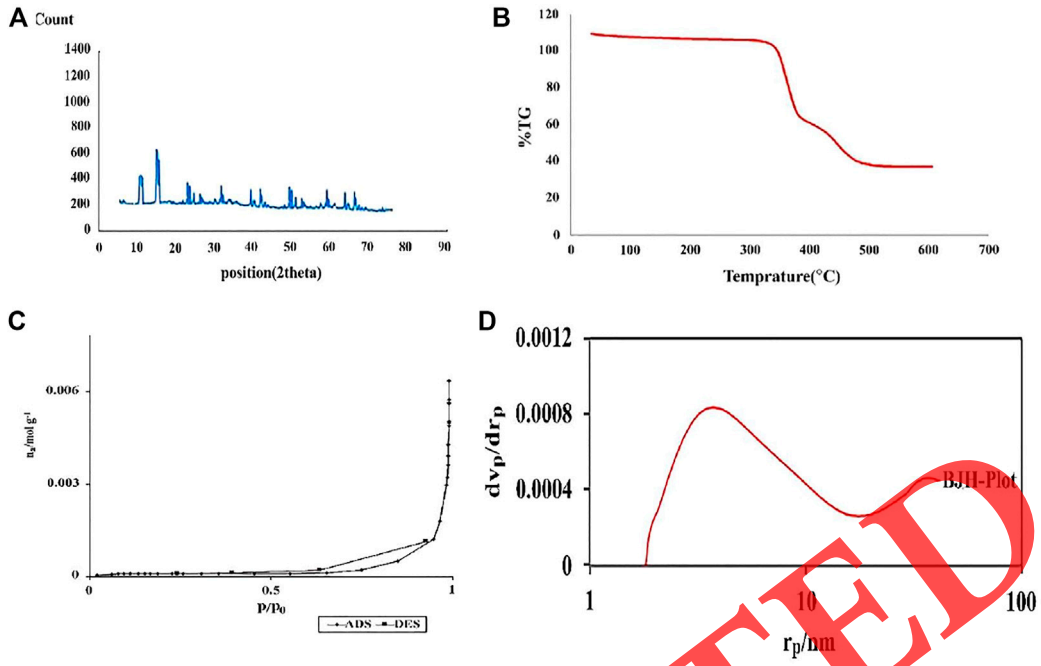

FIGURE 1 | XRD patterns in 2 theta angle of 0–90 **(A)**, TG curve in the range of 0–700°C **(B)**, N_2 adsorption/desorption behavior, **(C)** and BJH plot **(D)** for Ta-MOF/PEBA fibrous polymer.

used for the adsorption of CH_4 gas pollution due to their high specific surface area, stable chemical properties, high thermal stability, and significant porosity (Szczęśniak et al., 2018; Wu et al., 2019). Although the efficiency of these samples for trapping CH_4 is desirable, increasing their surface area properties for surface interaction between MOF nanostructures and CH_4 molecules is very important (Wang et al., 2018).

On the other hand, the use of biocompatible and biodegradable fibrous polymers has recently received attention. These compounds with various capabilities in the fields of medicine, engineering, and environment, depending on their properties, have various functions (Zhou et al., 2021; Hu et al., 2022; Li et al., 2022).

Fibrous nanostructures can be synthesized in various methods, and one of the most effective routes is electrospinning. This technique is rapidly developing from the single-fluid blending process (Li et al., 2021a; Homaeigohar and Boccaccini, 2022) to coaxial (Sapountzi et al., 2020; He et al., 2021a), side-by-side (Li et al., 2021b), tri-axial (Wang et al., 2020) and other complicated processes (He et al., 2021b; Luo et al., 2021). These processes expand the capabilities of electrospinning in creating novel functional nanomaterials by encapsulating different kinds of functional ingredients, including nanoparticles (Xue et al., 2021; Zhang et al., 2022).

If MOF nanostructures are integrated with fibrous polymers, their properties are expected to increase in particular, which will affect the performance of the samples (Sargazi et al., 2020). On the other hand, this also affects the specific surface of the final products, which results in the creation of compounds with high tendencies in the interaction between the surface of the structure and gas (Wang et al., 2019).

Systematic design of parameters in order to achieve maximum gas adsorption is very important. In non-systematic methods, the interaction between experimental parameters such as temperature, time duration, and pressure is not considered. In addition, achieving the optimal amount of CH_4 gas adsorption without considering the interaction between experimental parameters (temperature, time duration, and pressure) is a problem. Therefore, examining the effect of experimental parameters on CH_4 gas adsorption is a deep challenge (Pu et al., 2021).

In this study, for the first time, Ta-MOF/PEBA fibrous polymer nanostructures were synthesized by ultrasonic and electrospinning procedures. The resulting nanostructures were characterized by scanning electron microscopy (SEM) with energy-dispersive spectroscopy (EDS), thermogravimetric analysis (TGA), Brunauer–Emmett–Teller (BET) technique, and Fourier transform infrared spectroscopy (FT-IR). The resulting samples are used as a novel option for CH_4 gas adsorption. In order to deeply understand the amount of temperature, time duration, and pressure on CH_4 adsorption, a fractional factorial design has been used.

2 EXPERIMENTAL SECTION

2.1 Material Characterization

Ta $(NO_3)_5.6H_2O$, poly ether black amide (PEBA), and acetic acid were purchased from Sigma-Aldrich. All these chemicals were of

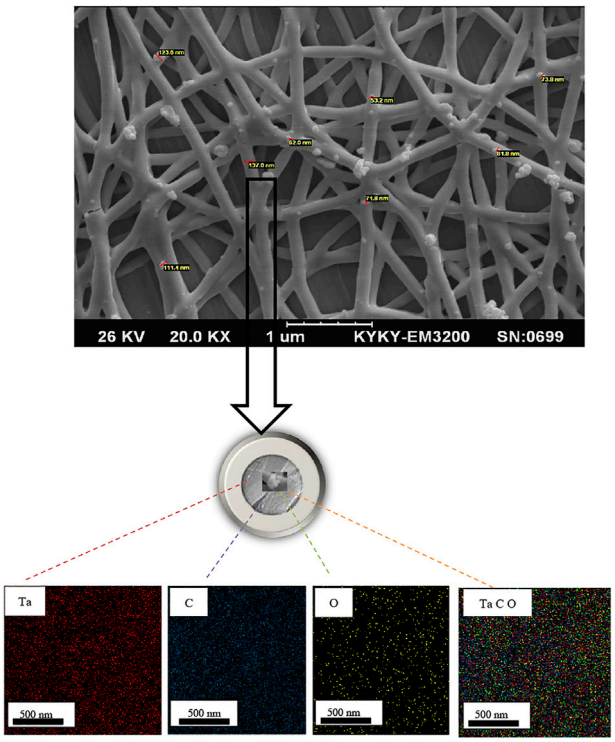

FIGURE 2 | SEM image with EDS elemental analysis of Ta-MOF/PEBA fibrous nanostructures.

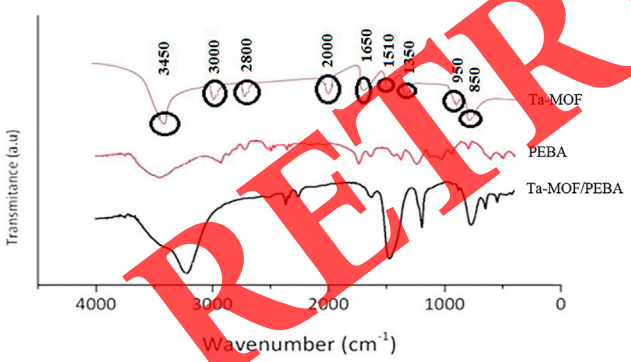

FIGURE 3 | FT-IR spectra of Ta-MOF, PEBA, and Ta-MOF/PEBA fibrous nanostructures.

analytical grade and were used without further purification. The microstructure behaviors of Ta-MOF/PEBA fibrous nanostructure samples were investigated by a scanning electron microscope (SEM, JEOL JSM6700F). Fourier transform infrared spectra (FT-IR, Nicolet IS10 IR spectrophotometer) were applied to characterize the related groups in the final structures.

The crystal behavior of the products was recorded by using a Scintag X1 diffractometer with monochromatized Cu–Kα irradiation (λ = 0.1540 nm) to recognize X-ray diffraction

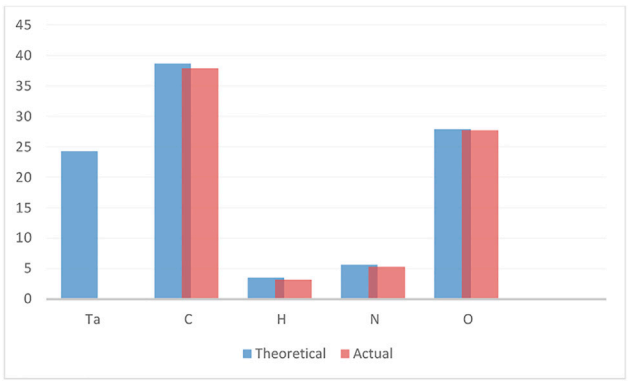

Element	Ta	C	H	N	O
Actual	-	37.86	3.19	5.29	27.71
Theoretical	24.27	38.67	3.52	5.64	27.90

FIGURE 4 | CHNS/O elemental analysis for Ta-MOF/PEBA fibrous polymeric nanostructures.

patterns. BET surface areas of Ta-MOF were investigated by a Micromeritics TriStar II 3020, Norcross, GA, gas adsorption analyzer. Thermogravimetric behaviors of the products were characterized by a DuPont TA Q50 analyzer.

2.2 Synthesis of Ta-MOF Nanostructures

In an ultrasonic typical synthesis, 2 mg of Ta $(NO3)_5.6H_2O$ and 6 mg of pyridine-2,6 dicarboxylic acid were dissolved in 50 ml of acetic acid. The resulting solution was placed in a magnetic stirrer for 40 min at 70°C. The mixture was transferred to an ultrasonic bath and irradiated under optimal ultrasonic conditions including temperature: 30°C, power: 150 W, and irradiation time: 70 min. Finally, white crystals of Ta-MOF were obtained after calcination under an argon atmosphere at 160°C.

2.3 Synthesis of Ta-MOF/PEBA Fibrous Polymeric Nanostructures

In order to synthesize Ta-MOF/PEBA fibrous polymeric nanostructures, the Ta-MOF nanostructures synthesized in the previous step (**section 2.2**) were dissolved in 25 ml of acetic acid. The final solution was homogenous under a magnetic stirrer at 150°C. The mixture was transferred into an electrospinning device at flow rate: 0.2 ml/h, voltage: 27 KV, PEBA concentration: 40 wt%, and spinning distance: 50 cm. Finally, the Ta-MOF/PEBA fibrous polymeric product was calcined at 180°C under an argon atmosphere.

2.4 CH_4 Gas Adsorption

To investigate CH_4 gas adsorption by Ta-MOF/PEBA fibrous polymeric nanostructures, a setup according to a voltametric method was used. The purity of CH_4 in the gas reactor was increased to 90% by the first generation of the GAMA PURIFICATION unit. The details of gas adsorption were reported in the previous work (Sargazi et al., 2020). The

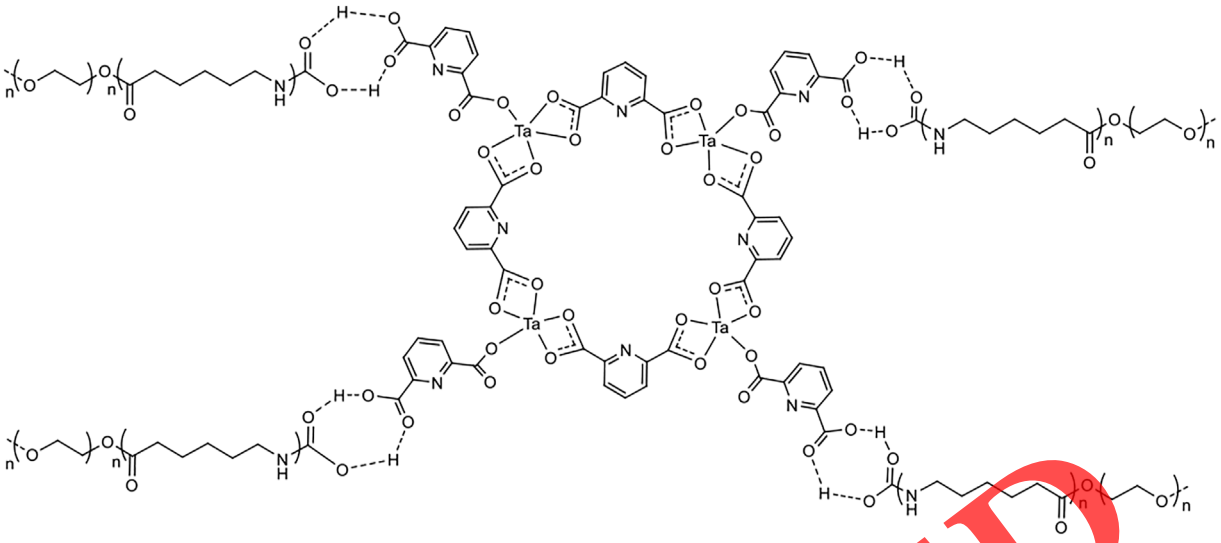

FIGURE 5 | Proposed structure for Ta-MOF/PEBA fibrous polymeric nanostructures.

TABLE 1 | Coded and non-coded ranges of the experimental parameters designed based on the fractional factorial method.

Level	Coded level	Uncoded level		
		Time duration (min)	Temperature (°C)	Pressure (bar)
Low	-1	20	20	1
Medium	0	35	40	2
High	+1	50	60	3

Coded formula: $\frac{X-\frac{x\ (high)+x(low)}{2}}{\frac{x(high)-x(low)}{2}}$, $x: -\omega \ldots, -3, -2, -1, 0, 1, 2, 3, \ldots, +\omega$

TABLE 2 | Randomized fractional factorial designs for CH_4 gas adsorption obtained by Ta-MOF/PEBA electrospun nanofibrous composite.

Runs	Std order	Center Pt	A (min)	B (°C)	C (bar)	REP	Adsorption (mmol/g)
a	9	1	−1	−1	−1	1	0.7
						2	0.6
b	5	1	0	−1	−1	1	1.4
						2	1.5
c	6	1	0	0	+1	1	4.1
						2	4.0
d	3	1	−1	+1	0	1	2.1
						2	2.0
e	2	0	0	0	0	1	3.7
						2	3.9

process was such that, first, a valve was installed between the dozer (storage reservoir) and tank (adsorption reservoir). Consequently, the number of CH_4 gas moles in the dozer was calculated using **Eq. 1**:

$$P_1V_1 = Z_1N_1RT \Rightarrow N1 = \frac{P1V1}{Z1RT}, \quad (1)$$

where P_1, N_1, R, T, and Z_1 show gas pressure, number of gas moles, general constant of gases, equilibrium temperature, and compressibility coefficient in the dozer, respectively. In the second step, the valve between the two reservoirs was opened and the Ta-MOF/PEBA fibrous products were placed inside the tank. Thus, as a result of transmission of gases into the tank, the amount of the CH_4 gas moles in tank could be calculated by **Eq. 2**:

$$P_2V_2 = Z_2N_2RT \Rightarrow N2 = \frac{P2V2}{Z2RT}, \quad (2)$$

where P_2, Z_2, and V_2 presented gas pressure, compressibility coefficient factor in the adsorption reservoir, and total volume of the adsorption and storage reservoirs, respectively. Finally, the

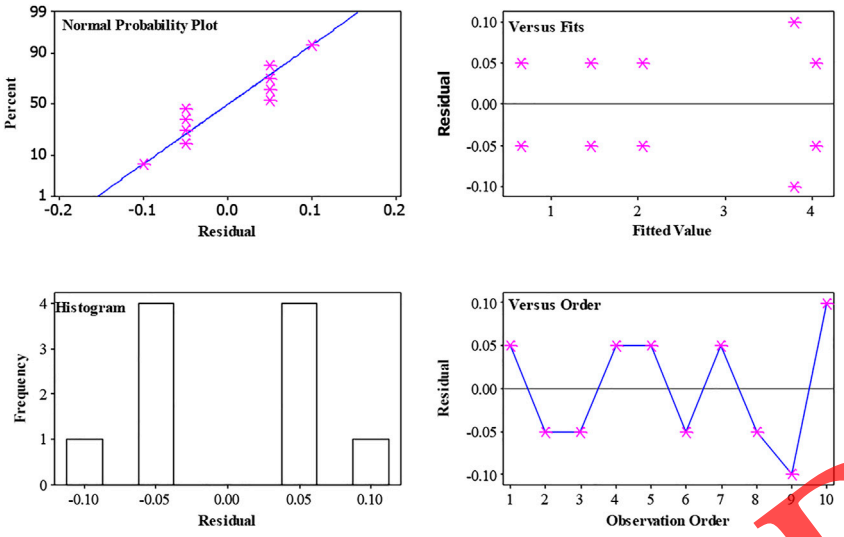

FIGURE 6 | Residual plot for different parameters of time duration **(A)**, temperature, **(B)** and pressure **(C)**.

TABLE 3 | Analysis of variance for CH_4 gas adsorption experiments by fractional factorial design.

Source	DF	Seq SS	Adj SS	Adj MS	P_{value}
A	1	7.3500	3.6038	3.60375	0.000
B	1	6.9769	1.4700	1.47000	0.000
C	1	2.0503	0.0625	0.0625	0.038
2-way interactions	3	1.1628	1.1628	1.16281	0.000
A*B	1	1.1628	1.1628	1.1628	0.000

gas moles adsorbed by the Ta-MOF/PEBA electrospun nanofibrous composite could be calculated by $n_{ADS}= n_1-n_2$.

3 RESULT AND DISCUSSION

3.1 Physico-Chemical Properties

XRD patterns of Ta-MOF/PEBA fibrous polymeric network are shown in **Figure 1A**. The existence of broad peaks in the final structures confirmed the nano-structural nature of these compounds. It can be related to the effective effect of ultrasonic and electrospinning routes on the final product (Sargazi et al., 2018).

Figure 1B shows the thermal stability of the Ta-MOF sample immobilized on the PEBA fibrous polymeric network from room temperature up to 600°C in order to study the thermal properties of the samples.

According to TG analysis, the main weight losses observed at 342°C can be attributed to the decomposition of frameworks in the network. As an important result, the Ta-MOF/PEBA fibrous polymeric sample has high thermal stability up to 340°C. It seems that the product developed in this study has more thermal stability than the pure Ta-MOF sample synthesized in the previous sample (Sargazi et al., 2018). Higher thermal stability of the electrospun products can be attributed to the incorporating physiochemical properties of the Ta-MOF and PEBA fibrous network. The synthesis of samples with high thermal stability provides the capability of final products in different areas.

The adsorption/desorption isotherm of the Ta/PEBA fibrous polymeric network samples is shown in **Figure 1C**. The adsorption/desorption behavior of this sample is similar to the third type of isotherm series, which showed mesoporous behavior for the products (Ebadi et al., 2009). According to the BET technique, the specific surface area of the sample is about 3700 m^2/g, which is significantly increased compared to the pure Ta-MOF sample (1784 m^2/g) (Sargazi et al., 2018). It seems that the participation of samples in fibrous networks and the effective effects of ultrasonic and electrospinning routes have significantly affected the specific surface area and porosity of the Ta-MOF/PEBA fibrous network. **Figure 1D** also showed the pore size distribution of the final products obtained by the BJH method. According to this method, Ta-MOF/PEBA fibrous nanostructures have mesoporous size distribution with a pore volume of 0.008 cm^3/g, which is in compliance with the data obtained from N_2 adsorption/desorption isotherms, while the pure Ta-MOF has a pore volume near 0.002 cm^3/g.

3.2 Morphology With Elemental Mapping

The microstructure results and morphology of the Ta-MOF/fibrous polymeric network are exhibited in **Figure 2**. As shown in this fig., the nanoparticles are well-immobilized in the network structure, which indicates effective combining of the Ta-MOF and fibrous structures. Also, the morphology of the samples is uniform, which confirms the effective effects of the synthesis route (Bai et al., 2021a; Bai et al., 2021b; Wang et al., 2021). EDS elemental analysis showed the distribution of related elements of Ta-MOF/PEBA nanostructures in the fibrous

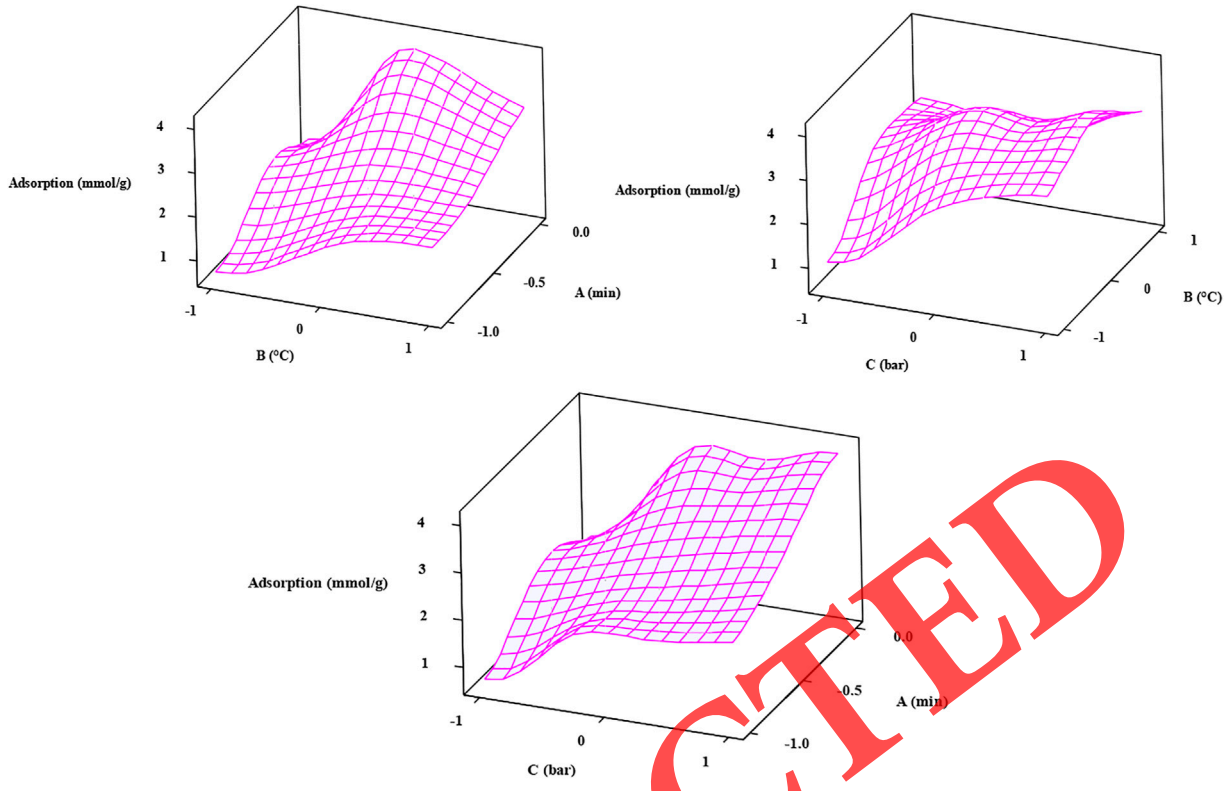

FIGURE 7 | Surface plot of CH_4 gas adsorption (mmol/g) vs. time duration [**(A)**-min], temperature [**(B)**-°C], and pressure [**(C)**-bar]. Data were reported as coded levels.

network. Also, this elemental mapping confirmed the homogenous distribution of samples in the final structures.

3.3 Proposed Structures of Ta-MOF/PEBA

Figure 3 shows the FT-IR spectra of Ta-MOF, PEBA, and Ta-MOF/PEBA fibrous nanostructures. In Ta-MOF and PEBA, the presence of a frequency close to 3500 cm^{-1} confirms the NH bonds related to the amine group in the structure (Tang et al., 2020). Also, the presence of bands at 2800 to 3050 cm^{-1} is attributed to the CH aromatic groups in the structures (Hu et al., 2021; Liu et al., 2022). In addition, absorption peaks in the range of 2000 cm^{-1} confirm the presence of various carbonyl groups in the structure. Due to the FT-IR spectrum of Ta-MOF/PEBA, all peaks related to the Ta-MOF and PEBA are observed in the final structure, which is a strong evidence for the successful synthesis of Ta-MOF/PEBA fibrous nanostructures. Also, CHNS/O elemental analysis of Ta-MOF/PEBA is presented in **Figure 4**. According to the data, the presence of related analysis was confirmed in the final structures. Based on FT-IR spectra and also CHNSO elemental analysis, the suggested structure of **Figure 5** was proposed for Ta-MOF/PEBA fibrous network nanostructures.

3.4 Systematic Study

In order to systematically study the process and investigate the effects of experimental parameters on CH_4 gas adsorption, the fractional factorial method has been used (Bruno Siewe et al., 2021). Experimental parameters include time duration (A), temperature (B), and pressure (C). The design of these parameters has been carried out in three levels (−1, 0, and +1). **Table 1** shows the arrangement of these parameters at three levels. The experiments under different conditions are presented in **Table 2**. All experiments were performed by two replications.

The residual plot of the experiments was used to investigate the scientific dispersion of experiments and their normal distribution (Huo et al., 2022; Jiang et al., 2021). As shown in **Figure 6**, the positive and negative levels are strong evidence for dispersion of the experiments on a regular basis. As a result, the dispersion of the experiments confirms the scientific distribution of the process (Wu and Hamada, 2011).

The effect of each of the experimental parameters of time duration, temperature, and pressure on the amount of CH_4 gas adsorption was investigated by analysis of variance (**Table 3**). As it is clear, temperature with a P_{value} of 0.000 has a significant effect on CH_4 gas adsorption. The effect of temperature on the adsorption of CH_4 gas is in accordance with the previous studies (Liu et al., 2020; Ullah et al., 2020). Pressure has also affected the performance of CH_4 gas adsorption (Xiao et al., 2009; Xu et al., 2021). According to the PV= znRT equation, the Ta-MOF/PEBA fibrous sample has a remarkable adsorption rate at high pressures. Therefore, the performance of Ta-MOF/PEBA

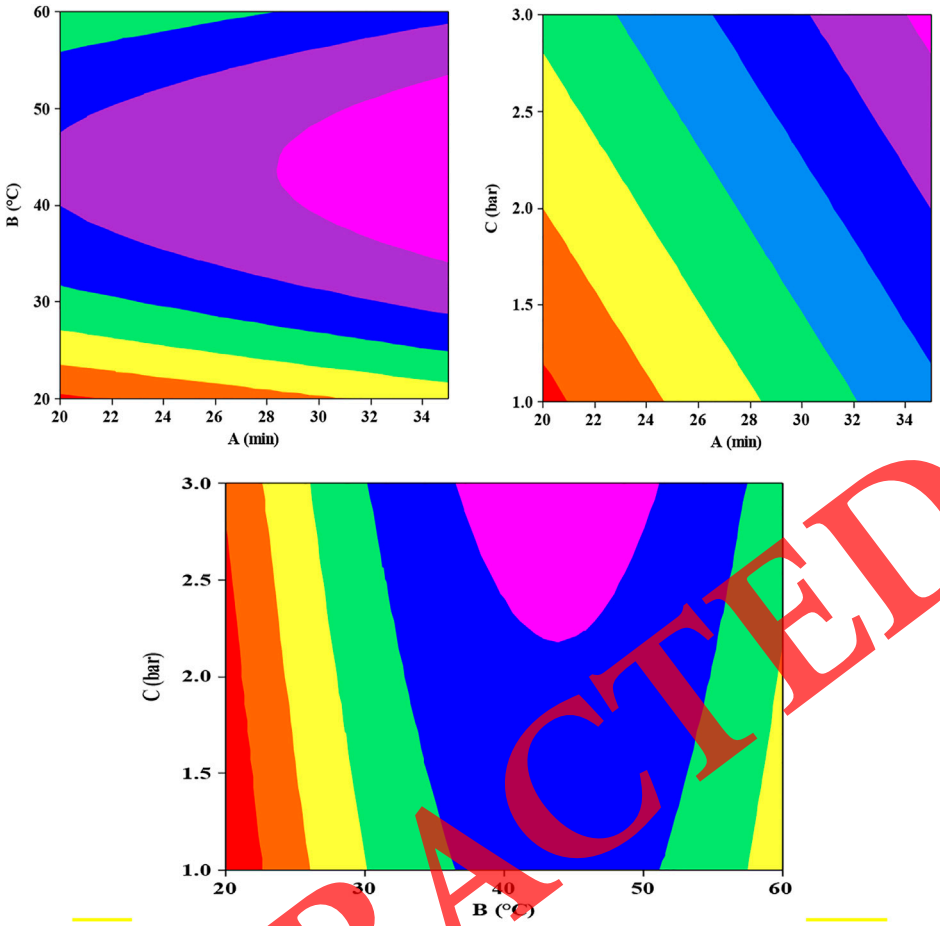

FIGURE 8 | Contour plot of CH_4 gas adsorption (color legend) vs. time duration **(A)**, temperature **(B)**, and pressure **(C)**. Data were reported as uncoded levels.

fibrous MOF in condition c is selected as optimal. Time duration also has a significant effect on CH_4 adsorption. With increasing time duration, more surface area of the nanostructures comes into contact with the gas, resulting in increased efficiency of CH_4 gas adsorption. Of course, it should also be taken into account that increasing the contact time to a certain extent can affect the amount of gas adsorption (Kirchstetter et al., 2001).

The surface plot has been used to investigate the relationship between experimental parameters of time duration (A), temperature (B), and pressure (C) and gas adsorption. As shown in **Figure 7**, by selecting different number of experimental parameters, desired values of CH_4 gas adsorption are obtained. This is a significant relationship between the experimental parameters in accordance with the results of **Table 2**. The counter plot also confirms this correlation for the experimental parameters and theatrical data (**Figure 8**). As an important result, optimization of the parameters theatrically facilitates the achievement of desirable conditions.

CONCLUSION

In this study, novel samples of Ta-MOF were synthesized under optimal ultrasonic conditions, including temperature: 30°C, power: 150 W, and irradiation time: 70 min. The resulting Ta-MOF samples were immobilized in PEBA fibrous networks by the electrospinning route. The obtained Ta-MOF/PEBA fibrous polymeric samples with desirable physicochemical properties such as significant specific surface area, high thermal stability, and small size distribution were used as novel candidates in the adsorption of gaseous pollutants. Factorial analysis has been used to investigate the effect of experimental parameters on the performance of products and also to systematically study the process. Analysis of variance confirmed the effects of time duration, temperature, and pressure on the efficiency of the Ta-MOF/PEBA fibrous sample in CH_4 gas adsorption. The compounds synthesized in this study open a new window to introduce effective biocompatible and biodegradable compounds for developing other gaseous pollutants.

DATA AVAILABILITY STATEMENT

The original contributions presented in the study are included in the article/Supplementary Materials; further inquiries can be directed to the corresponding author.

AUTHOR CONTRIBUTIONS

All authors listed have made a substantial, direct, and intellectual contribution to the work and approved it for publication.

REFERENCES

Afroz, R., Hassan, M. N., and Ibrahim, N. A. (2003). Review of Air Pollution and Health Impacts in Malaysia. *Environ. Res.* 92, 71–77. doi:10.1016/s0013-9351(02)00059-2

Bai, B., Jiang, S., Liu, L., Li, X., and Wu, H. (2021). The Transport of Silica Powders and Lead Ions under Unsteady Flow and Variable Injection Concentrations. *Powder Technol.* 387, 22–30. doi:10.1016/j.powtec.2021.04.014

Bai, B., Nie, Q., Wu, H., and Hou, J. (2021). The Attachment-Detachment Mechanism of Ionic/nanoscale/microscale Substances on Quartz Sand in Water. *Powder Technol.* 394, 1158–1168. doi:10.1016/j.powtec.2021.09.051

Bruno Siewe, F., Kudre, T. G., and Narayan, B. (2021). Optimisation of Ultrasound-Assisted Enzymatic Extraction Conditions of Umami Compounds from Fish By-Products Using the Combination of Fractional Factorial Design and Central Composite Design. *Food Chem.* 334, 127498. doi:10.1016/j.foodchem.2020.127498

Ebadi, A., Soltan Mohammadzadeh, J. S., and Khudiev, A. (2009). What Is the Correct Form of BET Isotherm for Modeling Liquid Phase Adsorption? *Adsorption* 15, 65–73. doi:10.1007/s10450-009-9151-3

He, H., Wu, M., Zhu, J., Yang, Y., Ge, R., and Yu, D.-G. (2021). Engineered Spindles of Little Molecules Around Electrospun Nanofibers for Biphasic Drug Release. *Adv. Fiber Mater.* 4, 1–13. doi:10.1007/s42765-021-00112-9

He, J., Xu, P., Zhou, R., Li, H., Zu, H., Zhang, J., et al. (2021). Combustion Synthesized Electrospun InZnO Nanowires for Ultraviolet Photodetectors. *Adv. Elect. Mater.* 8, 2100997. doi:10.1002/aelm.202100997

Homaeigohar, S., and Boccaccini, A. R. (2022). Nature-Derived and Synthetic Additives to Poly(ε-Caprolactone) Nanofibrous Systems for Biomedicine; an Updated Overview. *Front. Chem.* 9, 809676. doi:10.3389/fchem.2021.809676

Hu, X., Zhang, P., Wang, D., Jiang, J., Chen, X., Liu, Y., et al. (2021). AIEgens Enabled Ultrasensitive Point-Of-Care Test for Multiple Targets of Food Safety: Aflatoxin B1 and Cyclopiazonic Acid as an Example. *Biosens. Bioelectron.* 182, 113188. doi:10.1016/j.bios.2021.113188

Hu, Y., Yang, G., Zhou, J., Li, H., Shi, L., Xu, X., et al. (2022). Proton Donor-Regulated Mechanically Robust Aramid Nanofiber Aerogel Membranes for High-Temperature Thermal Insulation. *ACS Nano* 16 (4), 5984–5993. doi:10.1021/acsnano.1c11301

Huo, J., Wei, H., Fu, L., Zhao, C., and He, C. (2022). Highly Active $Fe_{36}Co_{44}$ Bimetallic Nanoclusters Catalysts for Hydrolysis of Ammonia Borane: The First-Principles Study. *Chinese Chemical Letters*. doi:10.1016/j.cclet.2022.02.066

Jiang, L., Wang, Y., Wang, X., Ning, F., Wen, S., Zhou, Y., et al. (2021). Electrohydrodynamic Printing of a Dielectric Elastomer Actuator and its Application in Tunable Lenses. *Compos. Part A Appl. Sci. Manuf.* 147, 106461. doi:10.1016/j.compositesa.2021.106461

Kirchstetter, T. W., Corrigan, C. E., and Novakov, T. (2001). Laboratory and Field Investigation of the Adsorption of Gaseous Organic Compounds onto Quartz Filters. *Atmos. Environ.* 35, 1663–1671. doi:10.1016/s1352-2310(00)00448-9

Li, D., Wang, M., Song, W.-L., Yu, D.-G., and Bligh, S. W. A. (2021). Electrospun Janus Beads-On-A-String Structures for Different Types of Controlled Release Profiles of Double Drugs. *Biomolecules* 11, 635. doi:10.3390/biom11050635

Li, T., Sun, M., and Wu, S. (2022). State-of-the-art Review of Electrospun Gelatin-Based Nanofiber Dressings for Wound Healing Applications. *Nanomaterials* 12, 784. doi:10.3390/nano12050784

Li, Y., Wang, D., Xu, G., Qiao, L., Li, Y., Gong, H., et al. (2021). ZIF-8/PI Nanofibrous Membranes with High-Temperature Resistance for Highly Efficient PM0. 3 Air Filtration and Oil-Water Separation. *Front. Chem.* 9, 1116. doi:10.3389/fchem.2021.810861

Liu, Y., Hou, J., and Wang, C. (2020). Absolute Adsorption of CH4 on Shale with the Simplified Local-Density Theory. *SPE J.* 25, 212–225. doi:10.2118/199344-pa

Liu, Y., Li, B., Lei, X., Liu, S., Zhu, H., Ding, E., et al. (2022). Novel Method for High-Performance Simultaneous Removal of NO and SO_2 by Coupling Yellow Phosphorus Emulsion with Red Mud. *Chem. Eng. J.* 428, 131991. doi:10.1016/j.cej.2021.131991

Luo, G., Zhang, Q., Li, M., Chen, K., Zhou, W., Luo, Y., et al. (2021). A Flexible Electrostatic Nanogenerator and Self-Powered Capacitive Sensor Based on Electrospun Polystyrene Mats and Graphene Oxide Films. *Nanotechnology* 32, 405402. doi:10.1088/1361-6528/ac1019

Mofarahi, M., and Gholipour, F. (2014). Gas Adsorption Separation of CO_2/CH_4 System Using Zeolite 5A. *Microporous Mesoporous Mater.* 200, 1–10. doi:10.1016/j.micromeso.2014.08.022

Murseli, S., Middlestead, P., St-Jean, G., Zhao, X., Jean, C., Crann, C. A., et al. (2019). The Preparation of Water (DIC, DOC) and Gas (CO_2, CH_4) Samples for Radiocarbon Analysis at AEL-AMS, Ottawa, Canada. *Radiocarbon* 61, 1563–1571. doi:10.1017/rdc.2019.14

Pu, Q., Zou, J., Wang, J., Lu, S., Ning, P., Huang, L., et al. (2021). Systematic Study of Dynamic CO_2 Adsorption on Activated Carbons Derived from Different Biomass. *J. Alloys Compd.* 887, 161406. doi:10.1016/j.jallcom.2021.161406

Rios, R. B., Stragliotto, F. M., Peixoto, H. R., Torres, A. E. B., Bastos-Neto, M., Azevedo, D. C. S., et al. (2013). Studies on the Adsorption Behavior of CO_2-CH_4 Mixtures Using Activated Carbon. *Braz. J. Chem. Eng.* 30, 939–951. doi:10.1590/s0104-66322013000400024

Sapountzi, E., Chateaux, J.-F., and Lagarde, F. (2020). Combining Electrospinning and Vapor-phase Polymerization for the Production of Polyacrylonitrile/Polypyrrole Core-Shell Nanofibers and Glucose Biosensor Application. *Front. Chem.* 8, 678. doi:10.3389/fchem.2020.00678

Sargazi, G., Afzali, D., and Mostafavi, A. (2018). An Efficient and Controllable Ultrasonic-Assisted Microwave Route for Flower-like Ta(V)-MOF Nanostructures: Preparation, Fractional Factorial Design, DFT Calculations, and High-Performance N_2 Adsorption. *J. Porous Mater* 25, 1723–1741. doi:10.1007/s10934-018-0586-3

Sargazi, G., Afzali, D., Mostafavi, A., and Kazemian, H. (2020). A Novel Composite Derived from a Metal Organic Framework Immobilized within Electrospun Nanofibrous Polymers: An Efficient Methane Adsorbent. *Appl. Organomet. Chem.* 34, e5448. doi:10.1002/aoc.5448

Szczęśniak, B., Choma, J., and Jaroniec, M. (2018). Gas Adsorption Properties of Hybrid Graphene-MOF Materials. *J. Colloid Interface Sci.* 514, 801–813. doi:10.1016/j.jcis.2017.11.049

Tang, X., Wu, J., Wu, W., Zhang, Z., Zhang, W., Zhang, Q., et al. (2020). Competitive-type Pressure-dependent Immunosensor for Highly Sensitive Detection of Diacetoxyscirpenol in Wheat via Monoclonal Antibody. *Anal. Chem.* 92, 3563–3571. doi:10.1021/acs.analchem.9b03933

Ullah, S., Bustam, M. A., Al-Sehemi, A. G., Assiri, M. A., Abdul Kareem, F. A., Mukhtar, A., et al. (2020). Influence of Post-synthetic Graphene Oxide (GO) Functionalization on the Selective CO_2/CH_4 Adsorption Behavior of MOF-200 at Different Temperatures; an Experimental and Adsorption Isotherms Study. *Microporous Mesoporous Mater.* 296, 110002. doi:10.1016/j.micromeso.2020.110002

Van Amstel, A. (2012). Methane. A Review. *J. Integr. Environ. Sci.* 9, 5–30. doi:10.1080/1943815x.2012.694892

Wang, H., Song, T., Li, Z., Qiu, J., Zhao, Y., Zhang, H., et al. (2021). Exceptional High and Reversible Ammonia Uptake by Two Dimension Few-Layer BiI3 Nanosheets. *ACS Appl. Mat. Interfaces* 13, 25918–25925. doi:10.1021/acsami.1c03261

Wang, M., Hou, J., Yu, D.-G., Li, S., Zhu, J., and Chen, Z. (2020). Electrospun Tri-layer Nanodepots for Sustained Release of Acyclovir. *J. Alloys Compd.* 846, 156471. doi:10.1016/j.jallcom.2020.156471

Wang, X., Xu, W., Gu, J. g., Yan, X., Chen, Y., Guo, M., et al. (2019). MOF-based Fibrous Membranes Adsorb PM Efficiently and Capture Toxic Gases Selectively. *Nanoscale* 11, 17782–17790. doi:10.1039/c9nr05795a

Wang, Y., He, M., Tian, Z., Zhong, H., Zhu, L., Zhang, Y., et al. (2018). Rational Construction of an Ssa-type of MOF through Pre-organizing the Ligand's Conformation and its Exceptional Gas Adsorption Properties. *Dalton Trans.* 47, 2444–2452. doi:10.1039/c7dt04867j

Wu, C. J., and Hamada, M. S. (2011). *Experiments: Planning, Analysis, and Optimization*. John Wiley & Sons.

Wu, D., Liu, J., Jin, J., Cheng, J., Wang, M., Yang, G., et al. (2019). New Doubly Interpenetrated MOF with [Zn_4O] Clusters and its Doped Isomorphic MOF: Sensing, Dye, and Gas Adsorption Capacity. *Cryst. Growth. Des.* 19, 6774–6783. doi:10.1021/acs.cgd.9b01193

Xiao, B., Byrne, P. J., Wheatley, P. S., Wragg, D. S., Zhao, X., Fletcher, A. J., et al. (2009). Chemically Blockable Transformation and Ultraselective Low-Pressure Gas Adsorption in a Non-porous Metal Organic Framework. *Nat. Chem.* 1, 289–294. doi:10.1038/nchem.254

Xu, P., Cao, J., Yin, C., Wang, L., and Wu, L. (2021). Quantum Chemical Study on the Adsorption of Megazol Drug on the Pristine BC3 Nanosheet. *Supramol. Chem.* 33, 63–69. doi:10.1080/10610278.2021.1938049

Xue, K., Si, Y., Xie, S., Yang, J., Mo, Y., Long, B., et al. (2021). Free-Standing N-Doped Porous Carbon Fiber Membrane Derived from Zn–MOF-74: Synthesis and Application as Anode for Sodium-Ion Battery with an Excellent Performance. *Front. Chem.* 9, 647545. doi:10.3389/fchem.2021.647545

Zhang, M., Song, W., Tang, Y., Xu, X., Huang, Y., and Yu, D. (2022). Polymer-Based Nanofiber-Nanoparticle Hybrids and Their Medical Applications. *Polymers* 14, 351. doi:10.3390/polym14020351

Zheng, B., Tong, D., Li, M., Liu, F., Hong, C., Geng, G., et al. (2018). Trends in China's Anthropogenic Emissions since 2010 as the Consequence of Clean Air Actions. *Atmos. Chem. Phys.* 18, 14095–14111. doi:10.5194/acp-18-14095-2018

Zhou, B., Liu, Z., Li, C., Liu, M., Jiang, L., Zhou, Y., et al. (2021). A Highly Stretchable and Sensitive Strain Sensor Based on Dopamine Modified Electrospun SEBS Fibers and MWCNTs with Carboxylation. *Adv. Electron. Mat.* 7, 2100233. doi:10.1002/aelm.202100233

Conflict of Interest: The authors declare that the research was conducted in the absence of any commercial or financial relationships that could be construed as a potential conflict of interest.

Publisher's Note: All claims expressed in this article are solely those of the authors and do not necessarily represent those of their affiliated organizations, or those of the publisher, the editors, and the reviewers. Any product that may be evaluated in this article, or claim that may be made by its manufacturer, is not guaranteed, or endorsed by the publisher.